

DesignCon 2019

How the Braid Impedance of Instrumentation Cables Impact PI and SI Measurements

Istvan Novak, Samtec
Istvan.novak@samtec.com

Jim Nadolny, Samtec
jim.nadolny@samtec.com

Gary Biddle, Samtec
Gary.biddle@samtec.com

Ethan Koether, Oracle
ethan.koether@oracle.com

Abstract

VNA instrumentation cables have a direct impact on low frequency, high dynamic range measurements. In this paper we explain these phenomena in the context of power integrity measurements. DC resistance and low frequency transfer impedance are relevant cable metrics which are shown to correlate with the measurement dynamic range.

Author(s) Biography

Istvan Novak is a Principle Signal and Power Integrity Engineer at Samtec, working on advanced signal and power integrity designs. Prior to 2018 he was a Distinguished Engineer at SUN Microsystems, later Oracle. He worked on new technology development, advanced power distribution and signal integrity design and validation methodologies for SUN's successful workgroup server families. He introduced the industry's first 25um power-ground laminates for large rigid computer boards, and worked with component vendors to create a series of low-inductance and controlled-ESR bypass capacitors. He also served as SUN's representative on the Copper Cable and Connector Workgroup of InfiniBand, and was engaged in the methodologies, designs and characterization of power-distribution networks from silicon to DC-DC converters. He is a Life Fellow of the IEEE with twenty-five patents to his name, author of two books on power integrity, teaches signal and power integrity courses, and maintains a popular SI/PI website.

Jim Nadolny received his BSEE from the University of Connecticut in 1984 and an MSEE from the University of New Mexico in 1992. He began his career focused on EMI design and analysis at the system and component levels for military and commercial platforms. His focus then shifted to signal integrity analysis of multi-gigabit data transmission. Jim is active within the technical community currently serving as a Technical Group chairman for IEEE P370, a standard focused on precision measurements of passive interconnect components. Jim is a frequent presenter at DesignCon with Best Paper awards in 2004, 2008, 2012, 2018 and has over 25 peer reviewed publications. At Samtec, Jim tracks technology trajectories via industry standards, MSAs and other collaborations. Jim enjoys cooking, fishing, hunting and golf in the hills of Pennsylvania.

Gary Biddle received his BS in Physics from University of Florida 1976 and MS in Physics from Penn State University 1991. His work experience includes high frequency VNA and EMI measurements, along with nearly 20 years of simulating PCB and interconnect structures. He has published several articles and holds several patents.

Ethan Koether is a Hardware Engineer at Oracle Corporation. He is currently focusing on system power-distribution network design, measurement, and analysis. He received his master's degree in Electrical Engineering and Computer Science from the Massachusetts Institute of Technology.

I. Introduction

For electrical interconnects, in addition to connectors and printed circuit boards, cables often have to be used to bridge the distance between circuit inputs and outputs. In the various applications, there is a diverse list of requirements and available solutions. For finished products, the size and cost of cables are important factors. For these high volume applications the cable can be optimized in terms of length and cable flexibility may be of less importance. If just a few connections are needed, the cable performance can be improved by switching to bulkier types with reduced losses and improved shielding. Ultimately semirigid or rigid coaxial cables can also be used. Laboratory measurement applications are different. Though cost of the cabling may be less important, many times we can not optimize (minimize) the length, resulting in a few-feet or several-feet long cables. While in volume applications the flexibility of cable may be a secondary requirement, in measurement applications, especially in lower frequency power distribution network measurements, flexibility is very convenient and therefore becomes an important quality metric. Luckily today a very large number of different cables are available, but we need to understand the potential unintended consequences when we decide which cable to use. As we will see in this paper, electrical parameters that may not even be on the data sheet will become important and may become the limiting factor. In this paper we will look at the impact of cable braid/shield performance on different measurement applications.

Figure I.1 shows a typical power-distribution network impedance measurement [1]. For low-impedance measurements, one-port connection schemes do not work, because among other limitations, the measured impedance may be less than the contact resistance. Three-cable measurement options can also be used, one port driving the test signal and two other ports measuring the DUT voltage and current. If we could use a one-port scheme, at low frequencies the cable shield performance may not be important, because the important parameter would be the cable loss, primarily driven by the center conductor, not the return. With two- and three-port measurement setups, however, the cable braids and shields form a ground loop. Unless the instrument provides the necessary isolation or common-mode rejection, this cable braid loop becomes a serious limitation.

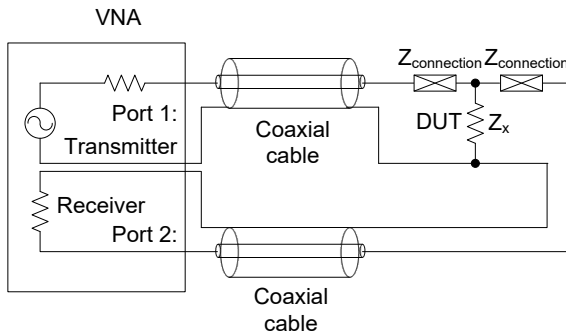


Figure I.1.: Typical connection scheme for measuring low PDN impedances.

Figure I.2 illustrates this error with measured data from [1]. The blue trace is the correct data; the DUT in this case was a 2.5 mOhm resistor. Instruments with floating or semi-

floating reference connections will show the correct results. Instruments where the returns of the two ports are tied together, will show erroneous reading (red trace).

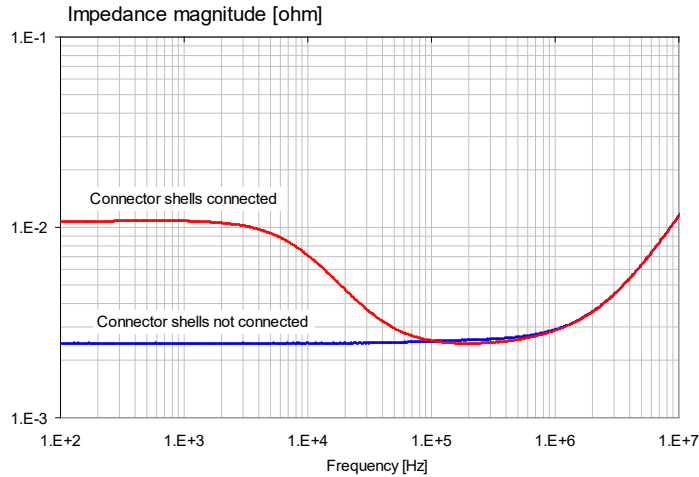


Figure 1.2.: Illustration of cable-braid error in PDN measurements.

Note that while this error has been known for a couple of decades [5], there are several further possibilities how the measured data may become corrupted. There are two typical scenarios. In one of them the upslope at the end of the frequency scale is created by damaged connector/cable joint or more frequently, the coupling between the loops associated with probe connections. In case of the illustration shown in *Figure 1.2*, this side effect was not present; the upslope of data correctly reflects the self inductance of the DUT piece.

The other typical data corruption occurs when the measuring cables have insufficient shielding, maybe because at low frequency PDN measurements the need for flexibility often wins over the need for good cable shield. With poorly shielded cables the measured response bottoms out even if we make sure that the measured impedance is much lower. To illustrate the effect of insufficient cable shield, we look at the VNA response when two 24-inch RG316 cables have solid shorts and the shorted cables are connected similar to what is shown in *Figure III.2.2*, except with solid metal caps on both cables. *Figure I.3* shows the setup on the top and the response on the bottom left. The noisy traces on both plots show the noise floor for comparison. When the two shorted ends are pushed against each other as shown on the photo, the response bottoms out approximately 10x above the noise floor. We don't reach the noise floor even with a large ferrite clamp on the cable, though the reading gets lower. As a comparison, the lower right plot shows the measured impedance of solid metal shorting caps; the response gradually reaches the noise floor.

In the simplest of signal-integrity (SI) measurement tasks, where we may need to check the reflection from a DUT (a one-port measurement) or the attenuation and delay of an interconnect (a two-port measurement), the cable-braid ground loop does not create a problem. Not only are DUT impedances in SI measurements much closer to the typical

50-ohm instrumentation impedance and therefore assessing the DUT impedance with one-port connection is readily doable, but also DUTs for SI measurements typically use connectorized joints, which is required to do more repeatable measurements.

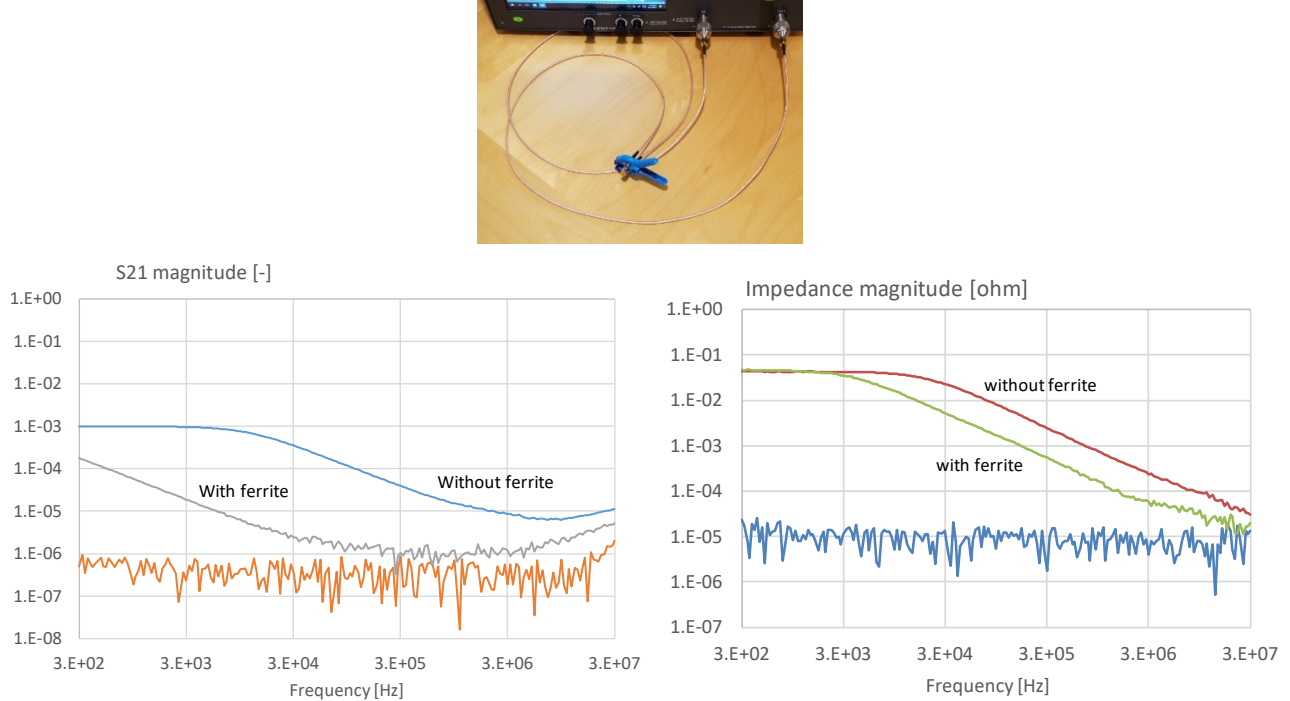


Figure I.3.: Setup to measure the effect of insufficient cable shield (top) and the resulting data with two 24-inch long RG316 cables (bottom left) and on two 1-m Sucoflex cables (bottom right).

Also, typical insertion losses of our interconnects tend to be low at low frequencies and therefore when we do two-port measurements, the signal from the cable-braid loop error becomes insignificant compared to the much larger useful signal. Furthermore, traditional vector-network analyzers used to start at 10 MHz frequency, where the cable-braid inductance already suppresses the cable-braid error to a large degree. For these reasons SI people usually do not experience the cable-braid error phenomenon. There is, however, one area of SI characterization, where this may become a limitation and hidden risk. It can happen when we measure crosstalk on multiple interconnects, where the return points are connected together. This would be the case in measuring near-end or far-end crosstalk in printed-circuit boards, packages and cable bundles, where the individual cable shields are tied together. *Figure I.4* is an illustration of this effect. The DUT is a simple two-sided test board with two microstrip traces (photo on the left). The figure compares near-end crosstalk with and without mitigating the cable-braid error. Note that even when we mitigate the cable-braid error, the crosstalk seems to start out with a finite low value at low frequencies. This is not a measurement artifact, rather the crosstalk through the shared return plane, which is real and is part of the DUT's response we need to measure. When we do not mitigate the cable-braid error, the low-frequency plateau may get much higher. This artifact will show up as an error in the steady-state response when we transform this frequency-domain data into the time domain. The

instrument for collecting data for *Figure I.3* was a low-frequency model [2], but high-frequency network analyzers have also become available with a sweep start frequency in the sub kHz range [3]. The same error shows up in the data when we do the same measurement directly in the time domain with a TDR/TDT instrument, but the much lower dynamic range of oscilloscopes usually masks this error.

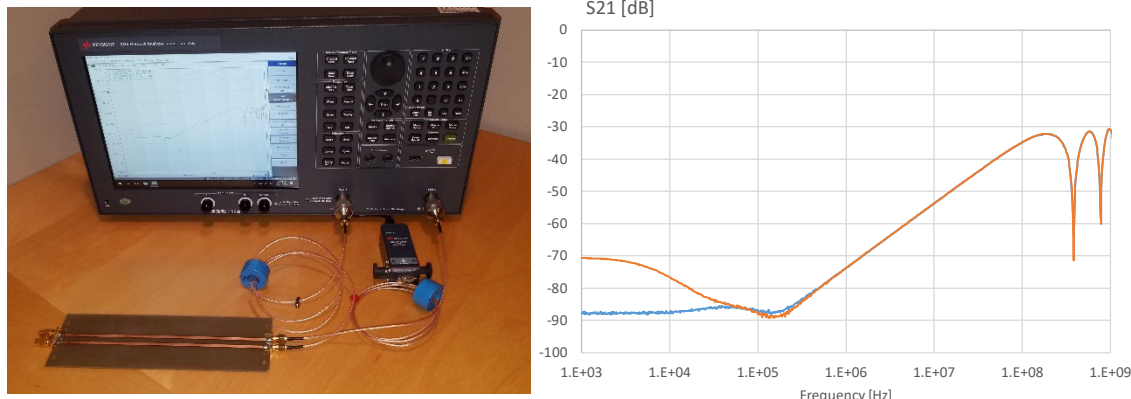


Figure I.4.: Effect of cable-braid error in crosstalk measurements on printed circuit boards. Photo of DUT on the left, measured near-end crosstalk with and without mitigating cable-braid error is shown on the right.

Last but not least, the cable shield performance is also important in EMC measurements. *Surface Transfer Impedance* or *Transfer Impedance* (TI) [4] is used to capture the impact, *Shielding Effectiveness* (SE) is also used on data sheets. Traditionally these parameters capture higher frequency effects, at a MHz or above, with the focus to see the interaction among the high-speed signals. As we will see later in the paper, cable braid error is related to the DC resistance of the instrumentation cable and it's transfer impedance.

II. The coupling mechanism

When using coaxial or twinax cables, the interaction between the wires inside the cable and the outside world happens not only through the connections at the end, but also through the shield. Dependent on the frequency and the construction of the shield, we get different degrees of interaction.

II.1 The cable shield

Coaxial cable shields can be broadly categorized as a braid, spiral wrap or a combination thereof. The creativity in combining and optimizing cable braids is a treatise in itself as the shield is a major cost and performance driver for the mature, high volume coax cable industry.

Braided shields are applied via an in-line process with a braiding machine which wraps multiple strands of very small wire in a precise geometry. This precise geometry is carefully controlled as it impacts both insertion loss and shielding. This topic is decades old with many excellent references [7], [8]. The braid can be characterized in terms of a

few simple parameters illustrated in Figure II.1. From an RF leakage perspective, the most important parameter is the aperture size associated with the braid weave.

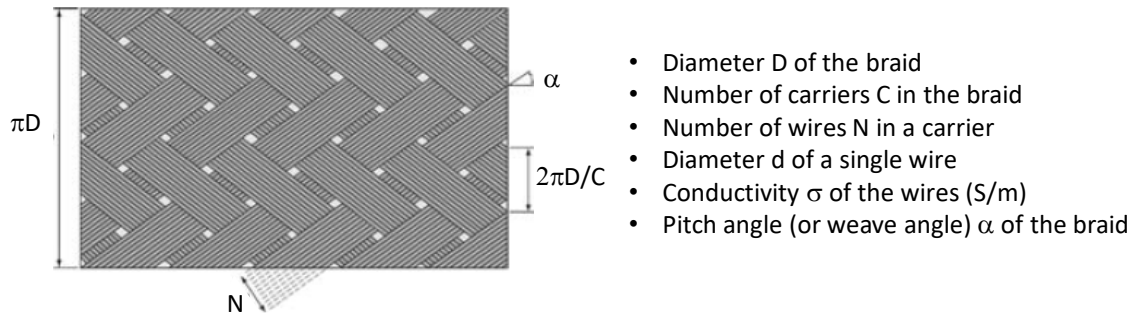


Figure II.1.: Cable Braid Parameters [7]

Cable braids are mechanically robust and are relatively easy to terminate with a coaxial connector. Coaxial connector attachment is typically a mechanical crimp process with care taken not to deform the relatively soft cable dielectric. From a manufacturing perspective, the braiding process is relatively slow and expensive in comparison to the inline dielectric extrusion process.

Spiral wrap shields have, in principle, no apertures, are less costly and lend themselves well to a high speed in-line manufacturing process. A thin foil, under carefully controlled tension, is precisely applied as the shield over an extruded core. Spiral shield materials are typically aluminized mylar although other foil materials are commonplace.

The major disadvantage of a spiral wrap shield is in its termination to a coaxial connector. The thin foil is mechanically frail in comparison to a braid and typically cannot be crimped. For the popular aluminized mylar shield, a helical aperture exists along the cable shield where the mylar overlaps the aluminized coating. The spiral wrap shield typically in electrical contact with a drain wire which is used for termination.

Combining these shields results in hybrid cable shields. RG-316 cable uses a double braid shield construction. High performing instrumentation grade coax cables often use a foil-braid combination which has the robust shield termination characteristics of a braid combined with the aperture free characteristics of a spiral wrap.

II.2 Transfer Impedance

Transfer impedance can be thought of as the AC impedance of the cable shield. More formally it is the ratio of the longitudinal voltage developed on one side of the cable shield to the current on the other side of the shield as illustrated in *Figure II.2*.

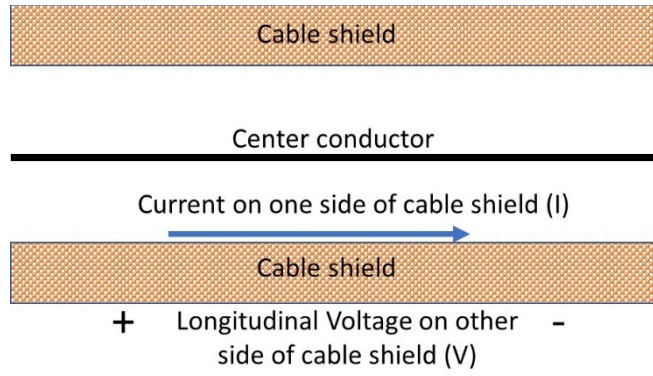


Figure II.2.: Transfer Impedance of a Coaxial Cable

As we go higher in frequency, small apertures in the cable braid become electrically significant. A distributed longitudinal inductance develops from the apertures resulting in an increasing longitudinal voltage. This increasing voltage is what drives the cable braid error at higher frequencies and gives rise to the shape of many cable transfer impedance curves. *Figure II.3* illustrates the apertures and their effect on transfer impedance. *Figure II.4* shows the classic shape of cable transfer impedance.

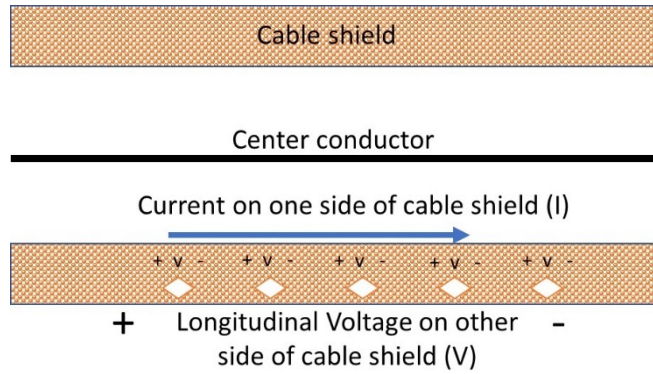


Figure II.3.: Apertures in Coaxial Cable Shield

Figure II.4 is helpful in understanding the mechanisms that shape the cable transfer response of braided cables, but this classic shape is by no means exhibited by all braided cables. If aperture leakage is small, the high frequency roll up may not be measurable. In contrast, if the aperture leakage is large, the skin effect regime may not be readily apparent. For these reasons measurements of transfer impedance are helpful in understanding the cable braid error.

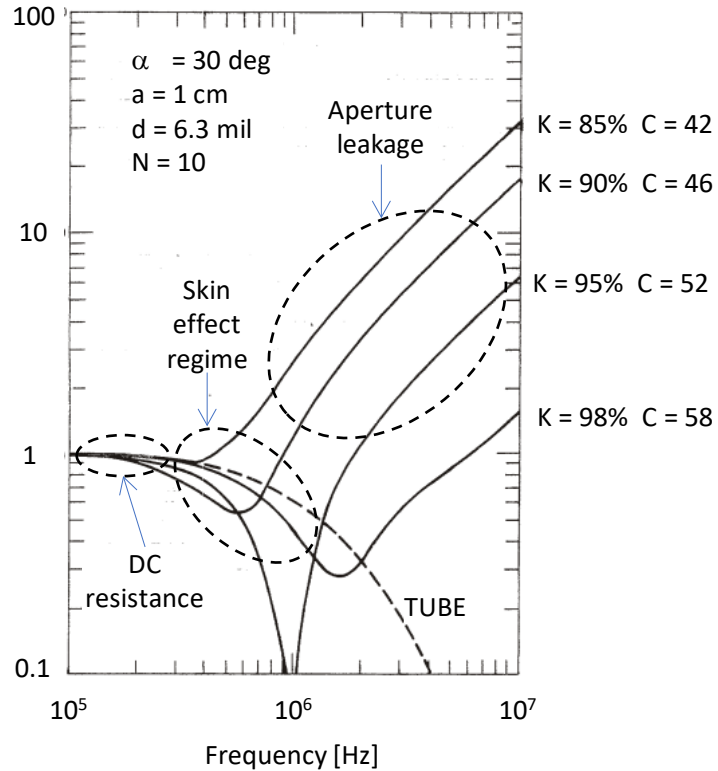


Figure II.4.: Transfer Impedance of Braided Cables [9]

III. Measurements

There are several important factors to measure about the cable braid and shield. We will start with the DC resistance, followed by the low-frequency transfer-impedance measurements and then we look at the high-frequency transfer impedance tests.

III.1 Rdc measurement

Per meter cable braid resistances are milliohms or tens of milliohms and therefore simple two-wire (or one-port) resistance measurements would create too much error and uncertainty. Instead, four-wire (or Kelvin) connections have to be used. There are four-wire resistance-measuring instruments readily available, but it is still a good idea to create fixtures to accommodate the connections to the coaxial connectors. Once we have fixtures, we can add precision power resistors so that we can measure current, add an adjustable voltage source and a voltmeter and we are ready to do four-wire Rdc measurements. A home-made setup is shown in *Figure III.1.1*. These fixtures have four 1-Ohm 1% power resistors connected series and parallel to form a 1-Ohm 1% 2W current-measuring resistor bank in series to the cable shield path. In series to the center connector of the cable there are four 10-Ohm 1% resistors configured to form a 10-Ohm current-measuring element. Banana receptacles provide easy connections to the power source and volt meter. As it will be explained below, we may want to measure the voltage drop along the cable braid/shield at different locations: the banana receptacles on

the fixture will provide data for the case when we want to measure the Rdc resistance over the entire path, including the connectors and their mating halves. If we need the DC resistance without the connectors, we can touch the exposed cable-braid with the measuring leads at the appropriate points. The second fixture on the bottom is labeled as ‘Current-limiting fixture’. It has a 10-ohmresistor, each, in series to the shield and center conductor paths. The purpose of these resistors is to limit the current and to allow a finer adjustment of current with the adjustable voltage regulator. The photo shows the scenario when a 2-foot coaxial cable is measured with a 1A DC current going through its shield.

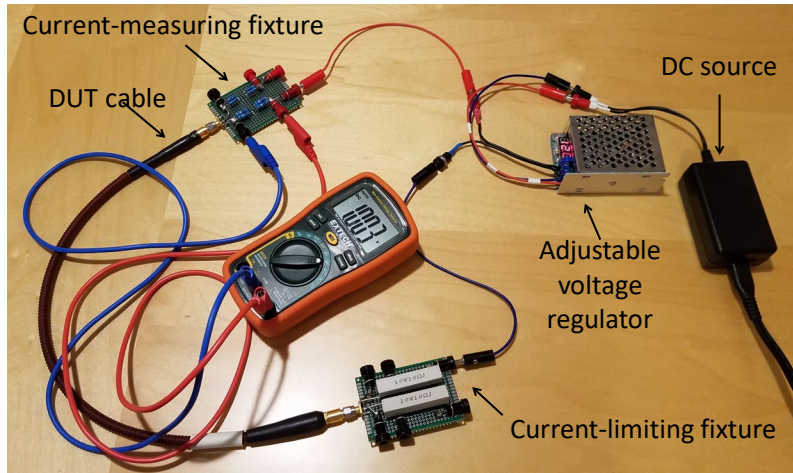


Figure III.1.1.: Home-made four-wire fixture to measure the DC resistance of braids and center wires of cables with SMA connectors.

In a real-life application, the DC resistance of the cable return path has multiple contributors: the resistance of the cable shield, connector at each end and the mating connector halves at each end. While the resistance of a solid metal connector piece can be very low, the contact resistance at each of the interfaces may add significant resistance to the cable-braid path. Eventually the same is true at the very end of the path, where the measuring cable continues in probes and the probe has to connect to the DUT. Just as a reminder, *Figure III.1.2* shows a two-port low-frequency measurement connection with wafer probes. The contact resistance of the ground blade is part of the ground-loop error that we need to deal with.

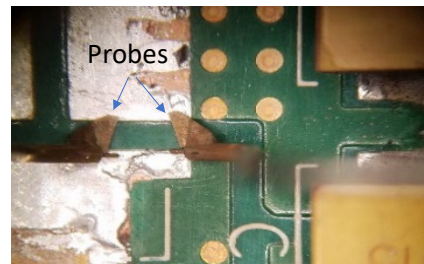


Figure III.1.2.: Wafer-probe PDN measurement.

Note that not only the connector contact resistance creates an uncertainty in the DC resistance: cables with any form of layered shield very likely will exhibit large uncertainty of DC resistance. For instance, when solid metal strips are used in a spiral shape around the cable, when we flex it, the spiral turns shift and move, changing the resistance. This can be seen with any instrument, whether we measure the voltage drop with a DC voltmeter or an oscilloscope or a network analyzer. *Figure III.1.3* is an illustration how it shows up on the network analyzer screen. The highlighted area shows the response due to relaxation due to prior flexing of the cable. This error diminishes over time and not shown in later sweeps if the cable is left alone.

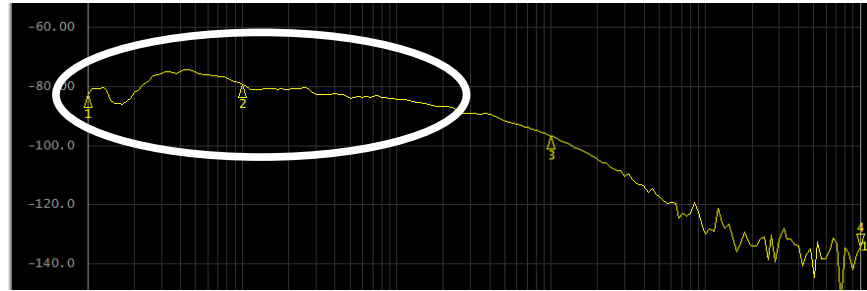


Figure III.1.3.: Changing DC resistance of cable shield over time due to prior flexing.

Table III.1.1 shows the DC resistance measurement results on some of the DUTs we used in this study.

Cable	Length [m] w, w/o connector	Rdc [mOhm] w/o connector
Red Gore	0.51/0.43	5.7
HP Grey	0.61/0.51	6.3
Storm	0.91/0.85	10.6
Sucoflex	1/0.92	12.7

Table III.1.1.: DC shield resistance of various coaxial cables.

III.2. Current measurements

The way how current flows in the cable braid plays a significant role in the Transfer Impedance (TI). The current can be measured in different ways. One typical setup uses the DUT conductor as one of the windings of a transformer, while the multiturn winding on a high-permeability core is part of the current probe. One of the current probes we used was a Tektronix P6021 current clamp for oscilloscopes. Its termination circuit requires a 1 MOhm load impedance, therefore an Agilent 41802A preamplifier was used to drive the VNA port. Home-made current-sensor pieces were used for calibration and

to check the current flow in various locations. *Figure III.2.1* shows the current sensor piece used for calibration. It is an insertable co-planar 50-ohm trace (cut in the middle) with a rectangular wire loop soldered to it. During the calibration of the current probe, it is connected to port 1 of the VNA, with its output terminated. The input impedance of this current sensor loop is shown on the right of *Figure III.2.1*. The impedance plots show the input reflection on magnitude and Smith charts, as well as the equivalent series resistance and inductance of the input impedance on the bottom. The sweep was set to run from 100 Hz to 100 MHz. Note that in spite of the added current-sensing loop, the input impedance is fairly well matched in the entire frequency range, ensuring good flatness for the test current.

With the current-measuring setup we want to check the current vs. frequency plots at various locations along the cables. The sketch of a Two-port Shunt-through impedance-measuring connection is shown in *Figure III.2.2*.

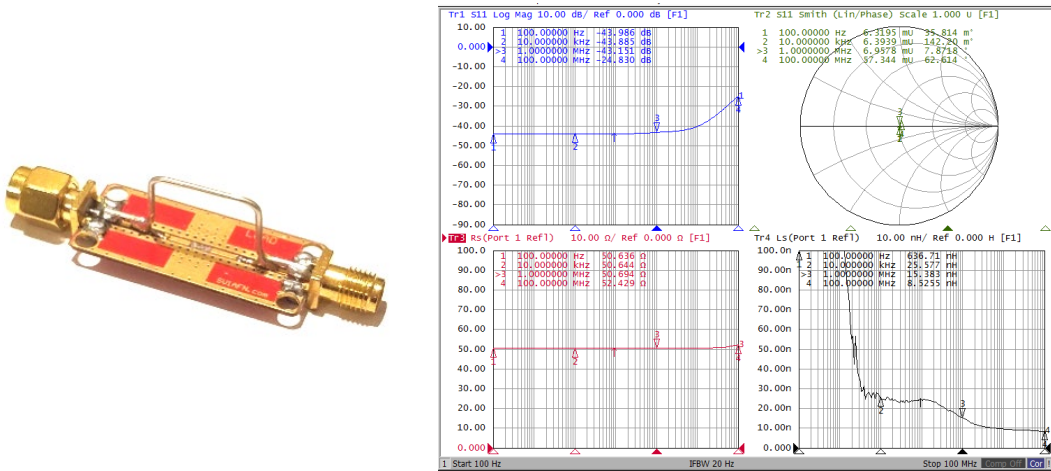


Figure III.2.1.: Closeup of a current sensor piece (on the left) and the return loss and R_s/L_s equivalent circuit values of the terminated current sensor (on the right).

Port 1 of the VNA drives the test signal and Port 2 picks up the voltage across the DUT. For this simplified connection we assume the extreme scenario: an ideal short to be measured as DUT. This means that the low-impedance DUT shorts both cables. To allow us to measure the current in that junction, a three-prong current-sensor element is inserted, the shape with brown lines between the two cables. The input of Port 2 cable is shorted by the fixture. The output of the Port 1 cable is shorted by a small rectangular loop and from the shorting loop a straight flexible wire connects to the shorted input of the Port 2 cable. This allows us to measure the current in this junction in three adjacent locations, 1, 2 and 3. *Location 1* is the output of the center conductor coming from Port 1. It carries the I_{c1} current, which is calibrated to a flat response. The current sensor at *Location 2* measures the current returning on the shield of Cable 1. *Location 3* shows the current jumping over from the shorted drive cable to the shorted receive cable. Along the structure we define four more locations and currents on the cables themselves. *Locations 4, 5, 6 and 7* allow us to measure the sum of the current in Cable 1 and Cable 2,

respectively, near the DUT and near the VNA ports. The blue horse-shoe shapes above the cables illustrate the occasional need to put ferrite clamps around the cables.

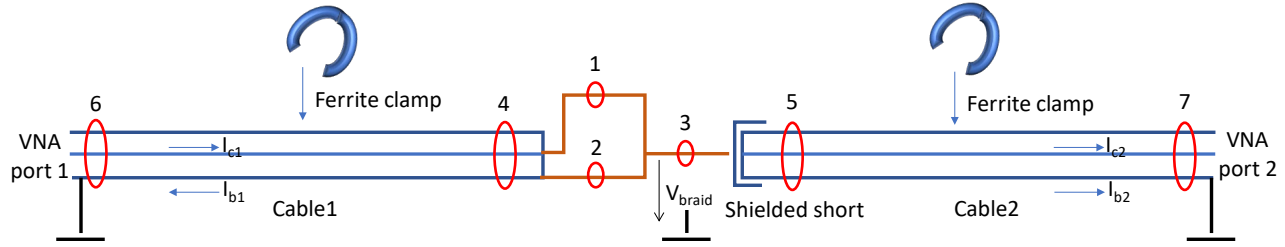


Figure III.2.2.: Schematics of current-measuring setup for Two-port Shunt-through impedance measurement.

For the actual implementation, two additional accessories were created, shown in *Figure III.2.3.* The termination block is required because Port 2, which normally would take Cable 2, is now used for the current probe. To ensure the same current distribution that we have in impedance measurements, we have to connect the braid of Cable 2 to the instrument return. To achieve this, the termination block combines the shells of Cable 1 and Cable 2 receptacles and allows for an optional 50-ohm load or short to be connected to the end Cable 2. To minimize the contact resistance, the shells of the T junctions are soldered together. The center pin of the left-side T-junction is removed, so the center wires of the two cables are not tied together. The three-prong current-sense element is shown on the right. The rectangular loop serves as a short, at the same time it allows us to measure the current flowing out of the center conductor and the current flowing into the braid. The inductance of the loop is small enough that in the frequency range of interest it does not alter the current in Cable 1 noticeably.

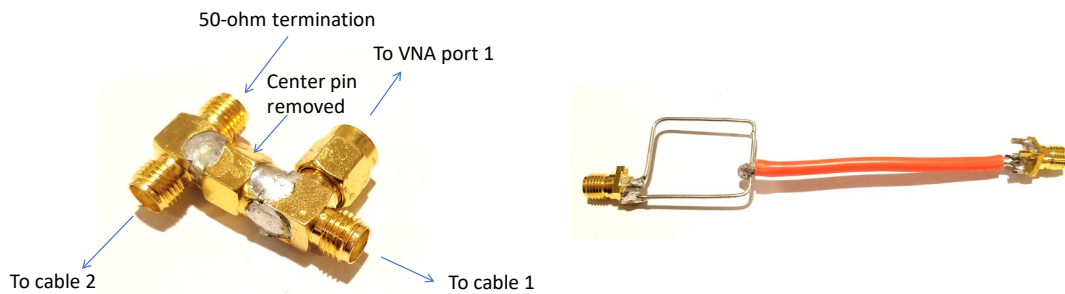


Figure III.2.3.: Photo of termination block (on the left) and current sensor element (on the right).

Figure III.2.4 shows the full setup: on the left during calibration, on the right during the testing of two 24-inch RG316 cables. The white toroid on the current-probe cable was necessary to suppress resonances on the probe cable. The test results are shown in *Figure III.2.5.*

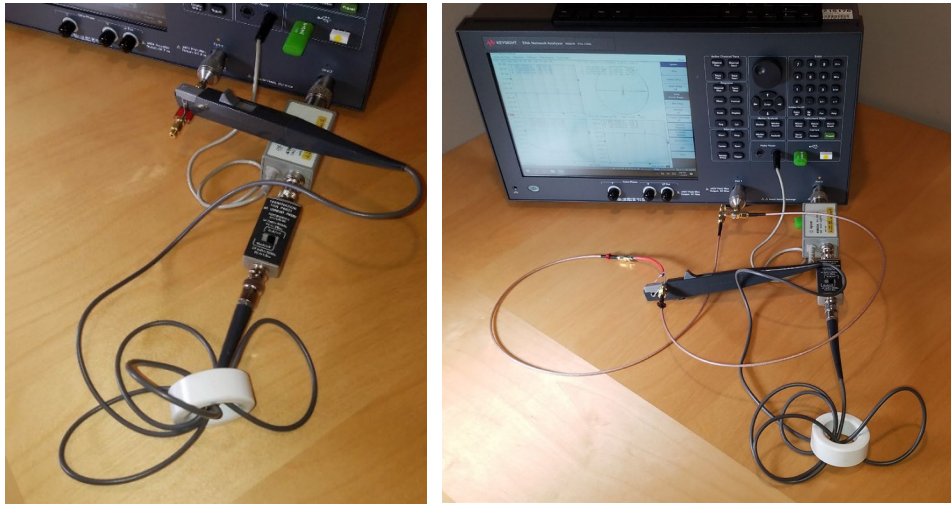


Figure III.2.4.: Current probe calibration setup (on the left) and DUT measurement (on the right). Note the white toroid on the current-probe cable; it is **not** on the DUT.

The I_{c1} response, measured at *Location 1* is flat at +6 dB value. The 6 dB increase with respect to calibration is due to the shorted cable, which attracts the shunt current of the source. At low frequencies the current at *Locations 2* and *3* are equally split. This is because we use the same length and type of cables, so their DC resistance is similar. As frequency goes up, the two responses start to deviate: response for *Location 2* gradually approaches +6 dB, whereas current at *Location 3* slopes down and it flattens out at -30dB level with no ferrite clamps.

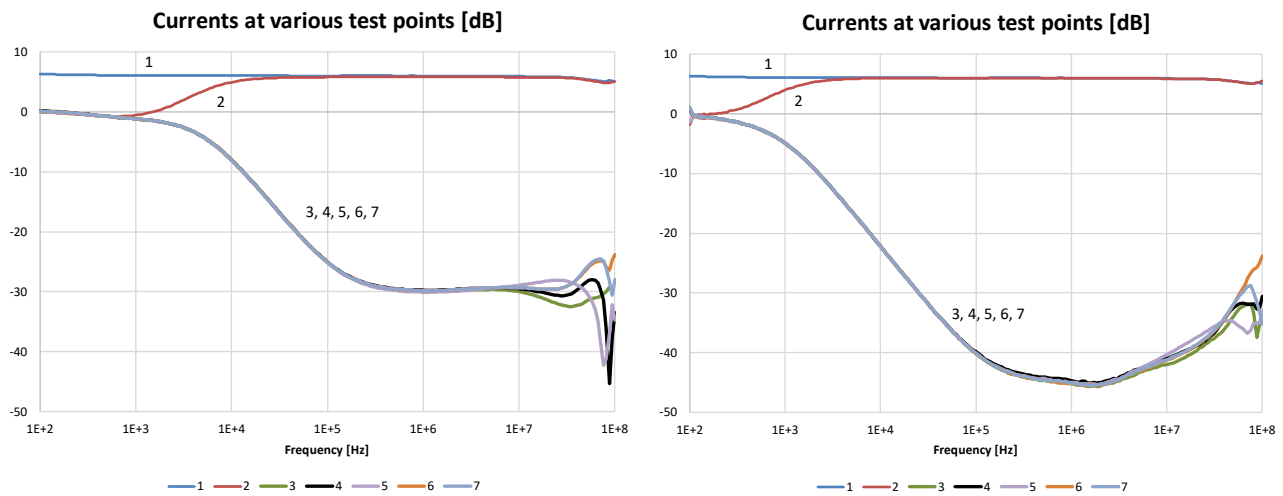


Figure III.2.5.: Relative current magnitude measured at the seven different test points along two 24-long RG316 cables. Response without (left plot) and with (right plot) ferrite clamps around the DUT cables.

With ferrite clamps added to both DUT cables, the main signatures remain the same, except responses at *Location 3* the response drops down to -46 dB before they start to slope up.

Note that measured responses at locations 4, 5, 6 and 7 run on top of response from *Location 3*. All response curves are smooth and no evidence of resonance below 10 MHz.

During the tests various cables and cable configurations were tested. In addition to the RG316 coax, several single-braid and braid-foil cables were tested. The main current signature and the relationship of frequency-dependent responses at the various locations were very similar. The default geometry was a single loose loop for each cable. The cables were also lifted off the table, straightening them out or coiling them up further. The 40-inch flexible cables were coiled up loosely in three turns, with and without ferrite clamps around the cables. The impact of an additional reference plane was also checked: a copper sheet, tied to the VNA connector shells, was placed under the cables. None of these geometry alterations changed the response by more than one or two dB, leaving the main signature unchanged.

III.4. Cable braid impedance test setup and results

A small test fixture was created with four right-angle PCB-mount SMA female connectors. Their connections were arranged in such a way that the impedance of the DUT cable (the cable with the three loose turns without a ferrite on the left and with ferrite clamp on the right) braid impedance is measured. *Figure III.4.1* shows the setup, *Figure III.4.2* shows the results.



Figure III.4.1.: Cable braid impedance measurement setup.

The screen capture of the VNA screen shows the impedance magnitude on logarithmic frequency scale from 100 Hz to 100 MHz. The lower left and right windows show the impedance real parts and extracted inductance, respectively. In all windows the lighter trace is the stored data with no ferrite clamp. Note that the extracted inductance is reasonably flat up to 10 MHz without ferrite, it has no signature that would explain the

inflection points in the response of *Figure I.3*. Note that this measured impedance is highly independent of the termination of the center wire.

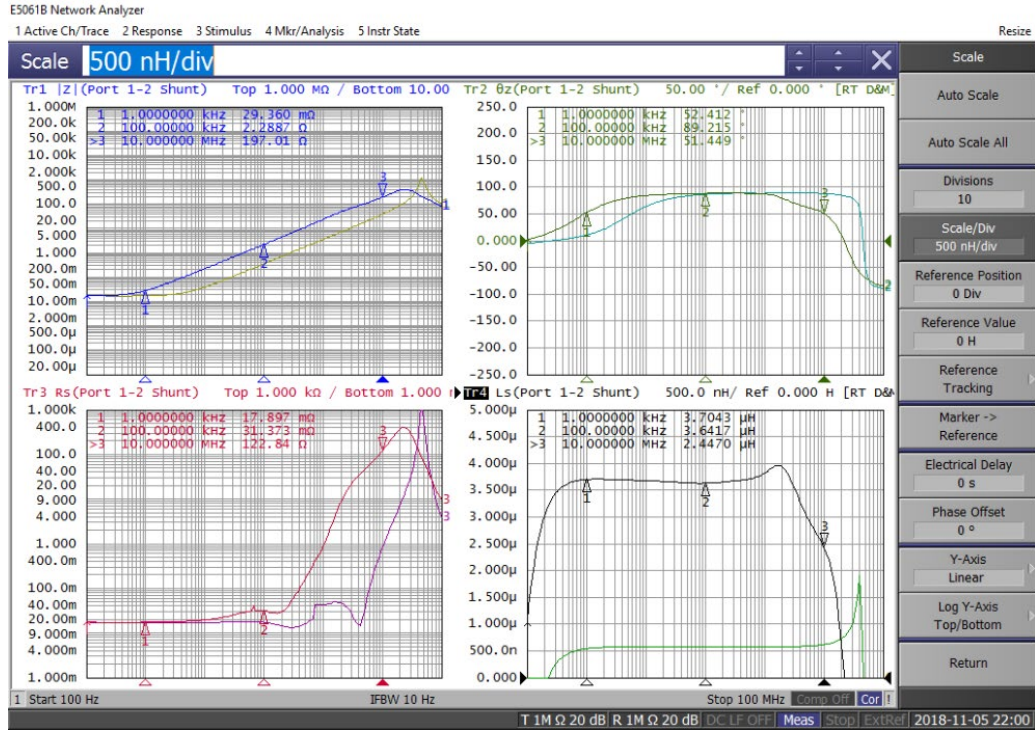


Figure III.4.2: Measured cable-braid impedance of a 24-inch RG316 cable.

III.5. High-frequency transfer impedance setup and results

To measure the high frequency transfer impedance of a cable we need the measured current on one side of the shield and the longitudinal voltage on the other side of the shield. The concept of an inner and outer transmission line is introduced here to illustrate the general test approach. Test fixtures typically have the cable braid acting as the common wall between the inner and outer transmission line as shown in *Figure III.5.1*. By exciting the inner transmission line with a constant voltage, the cable shield current can be extracted if we know the impedance of the inner transmission line. Voltage measured on the outer transmission line is due to the AC impedance of the cable shield.

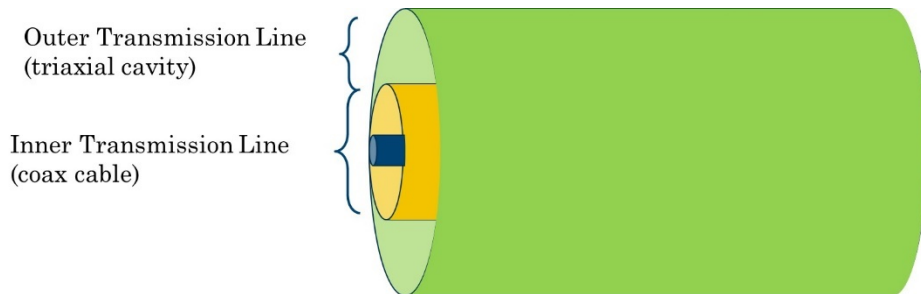


Figure III.5.1: Nested Test Fixture Concept for Transfer Impedance Measurements

There are several transfer impedance test methods including the line injection method (IEC 6253-4-6) and the triaxial method (IEC 62353-4-15)]. The quadriaxial test method was developed by Boeing and is shown in Figure III.5.2. With the quadraxial method the shield current is measured directly with a current probe. Triaxial cavities derive the shield current from a measured port voltage in a matched impedance environment.

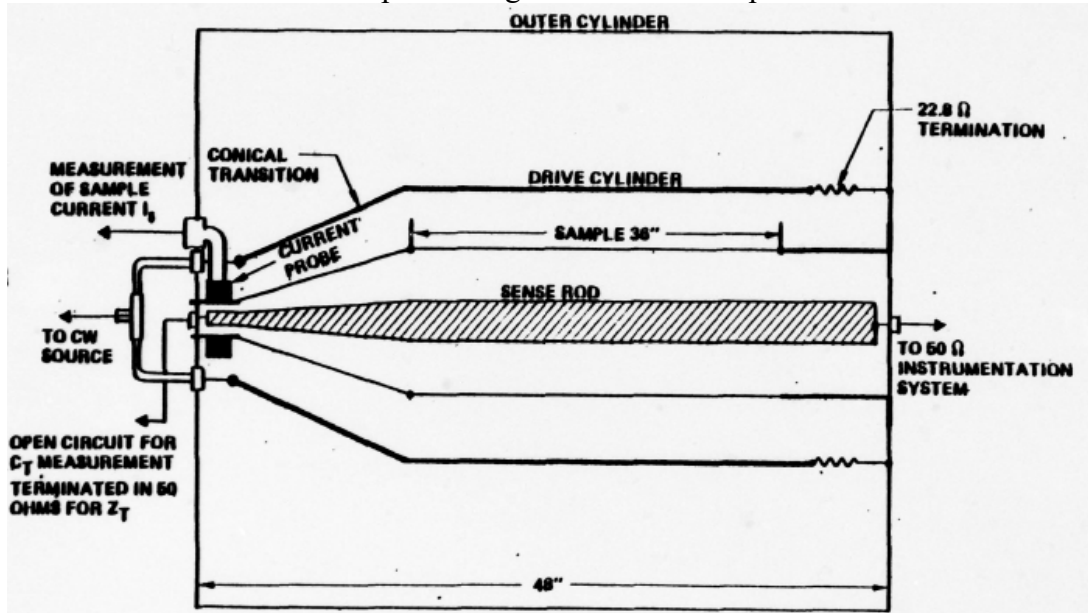


Figure III.5.2: Quadraxial Test Fixture for Transfer Impedance Testing

A quadraxial test fixture from Electronics Consulting Laboratory was used for the transfer impedance measurements in this paper.

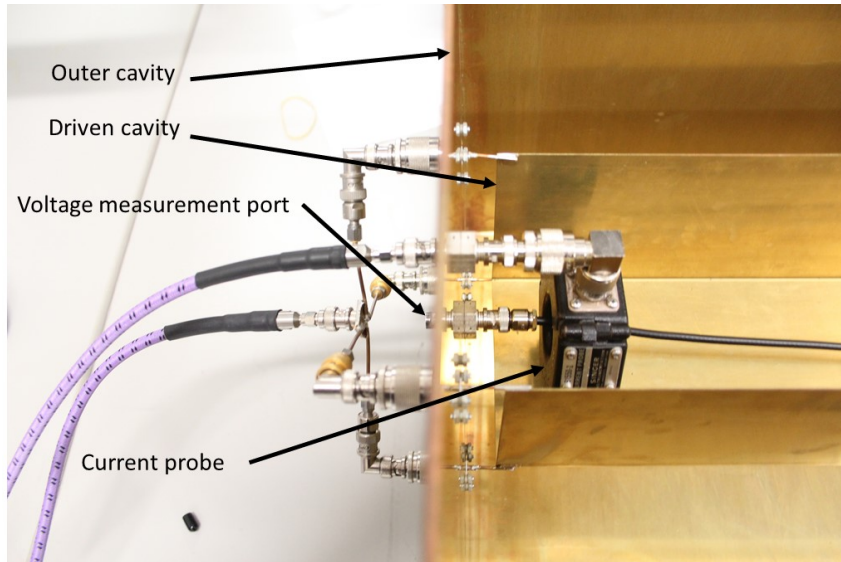


Figure III.5.3: Quadraxial Test Fixture Test Setup

A Keysight E5071C VNA was used for the transfer impedance measurements. A response-thru calibration establishes the measurement reference plane at the ends of the instrumentation cables. Two separate S21 measurements are made, one captures the current probe response and the second captures the voltage that is developed on the inner surface of the cable under test.

Figure III.5.4 shows the measured transfer impedance for two common cable type RG58 (single braid) and RG223 (dual braid). The data shows the general trend that the dual braid cable has lower transfer impedance and displays an increasing transfer impedance with frequency.

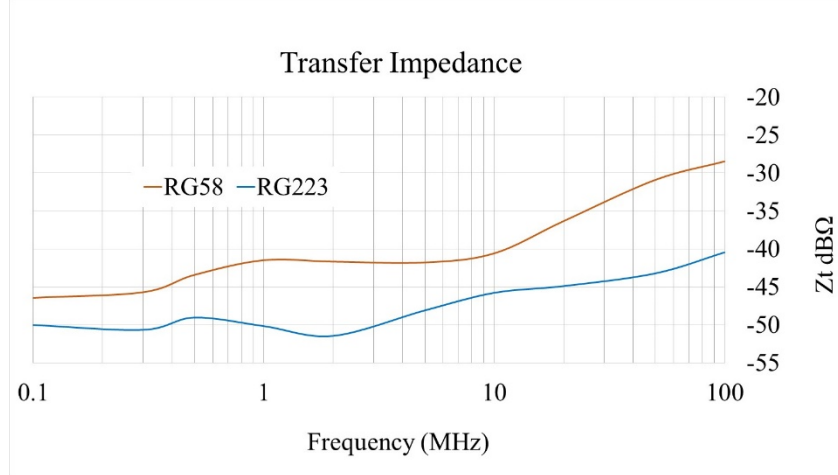


Figure III.5.4: Measured Transfer Impedance for RG58 and RG 223 in Quadraxial Test Fixture.

It must be mentioned that the quadraxial fixture used for this test is 27 inches long and accepts a 27 inch long cable. Unfortunately the cables tested were not 27 inches long, rather they were longer and had to be “coiled up” in the driven cavity. This led to a high degree of positional sensitivity which is the subject of current investigation. The margin of uncertainty is high for this data, on the order of 10 dB.

IV. Simulations and correlations

There are a number of models available for cable shield transfer impedance. Some of the models focus on the main signature of the cable-braid error [10], other models tend to capture the wide-band, frequency-dependent aspects of *Transfer Impedance* [6]. The motivation behind the high-frequency models is usually the need for immunity or susceptibility EMI simulations. The open-source model in [6] covers sufficiently wide frequency range so that the effect shown in *Figure I.3* could also be captured. However, empirical data suggest that the response plateau in *Figure I.3* is not created by coupling between the two cables or between the cables and surrounding objects through the braid, rather a self-contained lumped behavior of the cables. This led to the working assumption that the phenomenon at this relatively low frequency is created by the

imperfect inductive coupling between the cable's center wire and outer conductor. To test this hypothesis, a cascaded lumped cable model was created, which included frequency-independent RLGC elements and a non-ideal *Coupling coefficient* between the center-braid inductor and shield inductor elements. The model is shown in *Figure IV.1.*

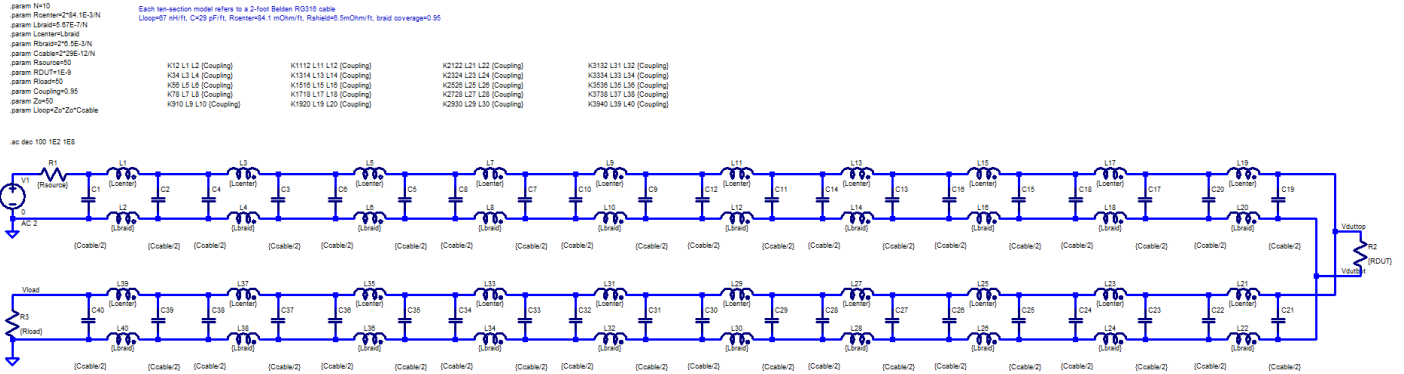


Figure IV.1.: LTSPICE model of cables. Parameter values are set for 2-foot RG316 cables.

The ten segments guarantee that each lump is electrically short and up to 100 MHz the model will approximate the distributed behavior well. The model has coupled inductors, one represents the center wire and the other represents the return or braid. The braid inductance is based on the measured inductance value from *Figure III.4.2*, and is in good agreement with inductance estimates for this length and diameter conductors. The default value for the center-wire inductance was set to equal the braid inductance. Different conductive losses were added separately to the center wire and braid. These were approximated by a frequency-independent DC resistance, based on data sheet and measured values. *Figure IV.2* shows the result the result.

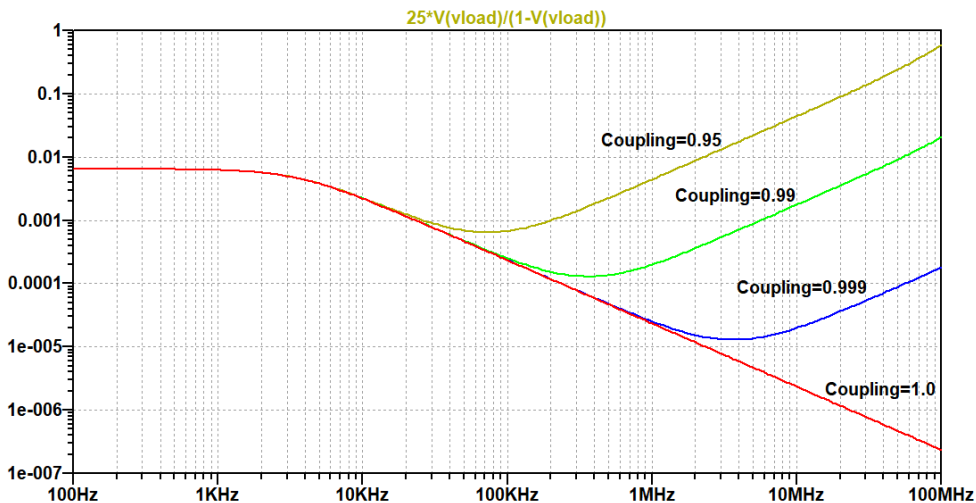


Figure IV.2.: Simulation result with the model shown on Figure IV.1.

The default value of *Coupling coefficient* was set to 0.95, which is the braid coverage value stated on the data sheet. The DUT impedance was set to practically zero (1E-9 Ohm). All items are parameterized, allowing easy sweeps of various parameters.

With these default values, first the *Coupling coefficient* was stepped over the values of 1.0, 0.999, 0.99 and 0.95. With ideal coupling of 1.0, the cable-braid error drops monotonically, similarly to what we see in measurements with cables having good shield. As the coupling coefficient is reduced, the mid-frequency plateau and the later rise of the response becomes more and more prominent, matching the signature we see in measurements.

When we sweep the braid inductance over a decade of values (*Figure IV.3*), the minimum value of the response does not change, but (as expected), the low-frequency corner of the response, which is determined by the $L_{\text{braid}}/R_{\text{braid}}$ time constant, moves linearly with it.

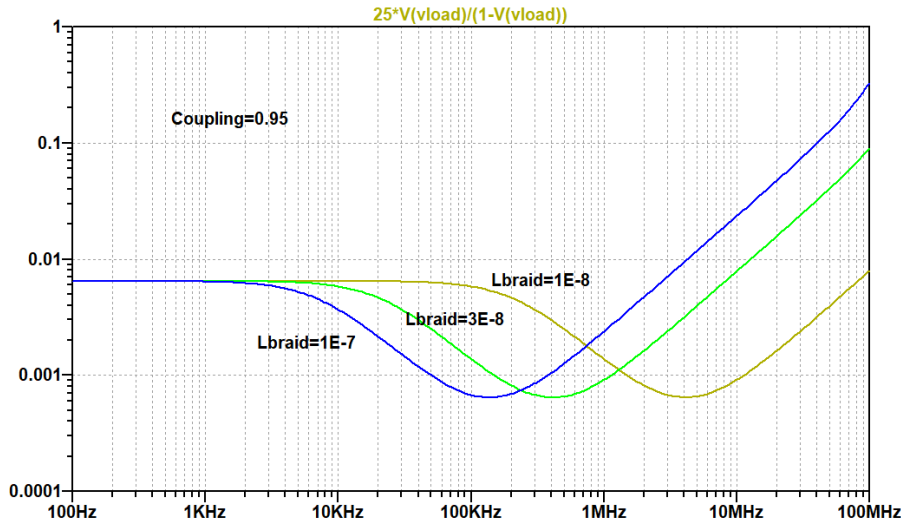


Figure IV.3.: Simulation result with the model shown on Figure IV.1 with cable braid inductance stepped over a 10:1 range.

Figure IV.4 illustrates and confirms the empirical finding that the capacitance (or characteristic impedance) of the cable has no impact on this low-frequency behavior. For this cable the capacitance or characteristic impedance has an impact on the response only above 30 MHz. If we keep the braid inductance at its default value, but step the inductance of the center wire over an unrealistically large 10:1 range at steps 1E-8, 5E-8, 1E-7 H (see *Figure IV.5*), we can observe that the upslope shifts to the right and the minimum value of the response shifts lower with increasing inductance values. In reality, the center-wire partial self inductance is not significantly different from the braid inductance, so this plot is used only to show us the trend.

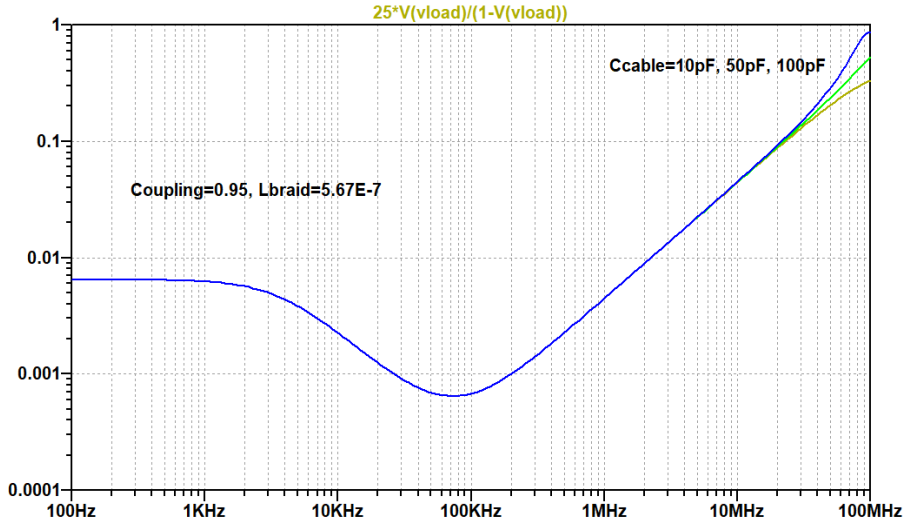


Figure IV.4.: Simulation result with the model shown on Figure IV.1 with cable capacitance stepped over a 10:1 range.

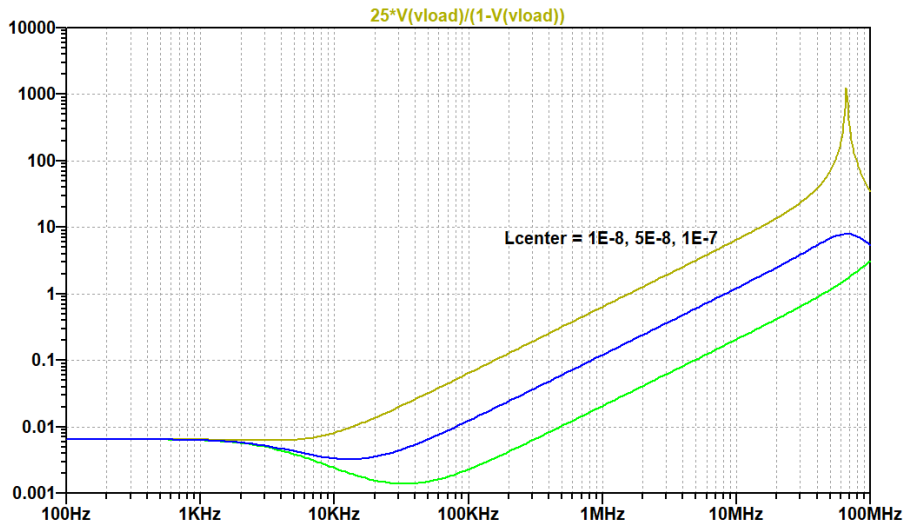


Figure IV.5.: Simulation result with the model shown on Figure IV.1 with cable center wire inductance stepped over a 10:1 range.

The cable braid DC resistance has a direct impact on the error response. When only the resistance is swept, but the braid inductance is kept constant, the braid resistance-inductance cutoff frequency changes, as well as the DC error. With these changes the minimum value of the error response also shifts. This is shown in *Figure IV.6*.

As expected, the center wire resistance of the cable has negligible impact on the main error signature. The resistance, even though could be an order of magnitude higher than

the braid resistance, is in series to the 50-ohm terminations, moreover in practical measurements its effect is removed by the calibration.

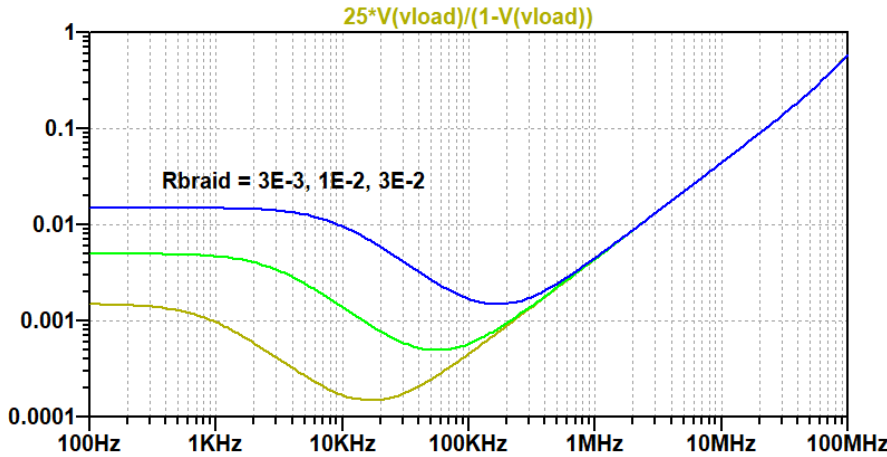


Figure IV.6.: Simulation result with the model shown on Figure IV.1 with cable center wire inductance stepped over a 10:1 range.

V. Summary and conclusions

In this paper we showed that the finite shielding effectiveness or transfer impedance of the cable creates noticeable errors in both SI and PI measurements. In both cases the error shows up when shields of two measurement cables form a ground loop and the measured quantity is low at low frequencies. In SI measurements this happens when we measure crosstalk on printed circuit boards or bundled cables and it can lead to incorrect low-frequency extrapolations when frequency-domain response is transformed into time-domain results. The error is more pronounced and more problematic in PI measurements if we need to measure very low impedances with two-port shunt-through measurement scheme. The finite transfer impedance of the cable creates a low-frequency error, which - for good shields- monotonically drops above the cable braid cutoff frequency. For cables with weaker shields the error response reaches a minimum, followed by an upslope, just as it is the case with the transfer impedance response. It was shown, however, that at low frequencies the error signature at medium frequencies is not the result of the interaction between the two cables through the air, rather it is a lumped phenomenon confined to within the cable and it is driven by the loosening coupling between the inductances of the center wire and the braid. With ideal tight coupling the coupled inductance ‘translates’ the common-mode error created by the cable braid loop to differential signal and this common-mode to differential-mode conversion gets weaker with non-ideal coupling between the inductances.

References

- [1] “Accuracy Improvements of PDN Impedance Measurements in the Low to Middle Frequency Range,” DesignCon 2010.
- [2] Keysight E5061B VNA, <https://literature.cdn.keysight.com/litweb/pdf/5990-4392EN.pdf?id=1790097>
- [3] Keysight N5245B VNA <https://literature.cdn.keysight.com/litweb/pdf/N5245-90028.pdf?id=2871559>
- [4] S. Sali, “An Improved Model for the Transfer Impedance Calculations of Braided Coaxial Cables,” IEEE Transactions on EMC, Vol. 23, No.2, May 1991
- [5] “Measuring MilliOhms and PicoHenrys in Power-Distribution Networks,” DesignCon 2000, http://www.electrical-integrity.com/Paper_download_files/DC00_MeasuringMiliohms.pdf
- [6] S. Greedy, et.al, “Open Source Cable Models for EMI Simulations,” IEEE EMC Magazine, Volume 7, Quarter 3.
- [7] “Uncertainties in Cable Transfer Impedance”, JL Rotgerink, et.al, 2018 IEEE EMC Magazine, Volume 7, Quarter 3
- [8] “Transmission Line Matching and Crosstalk”, K. Kaiser
- [9] “Shielding Effectiveness of Braided Wire Shields”, Instruction Note 172, E. F. Vance, 1974
- [10] Steve Sandler, “Designing and Measuring 100uOhm Power Rails,” EDICON 2018, October 2018, Santa Clara, CA